Heat and Mass Transfer in MHD Stagnation-point Flow over a permeable Stretching/Shrinking Sheet in the Presence of Radiation Effect, Soret Effect and Slip Parameter

Fatin Nabila Kamal[1,a] and Khairy Zaimi[1,b]

[1]Institute of Engineering Mathematics, Universiti Malaysia Perlis,
Pauh Putra Campus, 02600 Arau, Perlis, Malaysia.

ABSTRACT

The numerical solution of steady two-dimensional magnetohydrodynamic (MHD) stagnation-point flow over a permeable stretching/shrinking sheet with radiation effect, Soret effect and slip parameter is considered in this study. The mathematical model formulation was done by reducing the governing partial differential equations to a system of ordinary differential equations by using a similarity transformation. Next, the ordinary differential equations were solved numerically using bvp4c functions and shooting method. Numerical results obtained are presented in tables and graphs, showing the effects of slip parameter and Soret effect on the flow field, heat and mass transfer characteristics. The dual solutions are found to exist in a certain range of parameters, which is shrinking case, while the solution is unique for the stretching case. It is observed that as the slip parameter increases, the skin friction coefficient decreases while the Nusselt number and Sherwood number increases. It is observed that the Sherwood number decrease as the Soret effect increase. Results also indicate that slip effect widens the range of stretching/shrinking parameter for which solution exists.

Keywords: Stagnation point flow, stretching/shrinking sheet, radiation effect, Soret effect, slip parameter and suction/injection.

1. INTRODUCTION

The stagnation-point flow is described as the fluid motion near the stagnation region, which exists for both cases of a fixed or moving body in a fluid. The highest pressure, the highest heat transfer and the highest rate of mass decomposition is encountered in the stagnation region. The study of stagnation-point flow has gained attention of many researches due to its wide range of applications on several industrial process such as cooling of electronics devices by fans, cooling of nuclear reactors during emergency shutdown, glass blowing, the cooling and drying of papers and textiles, etc. Hiemenz[1] is the first researcher who studied the two-dimensional stagnation flow passed through a fixed surface and obtained exact solution of the Navier-Stokes equations using similarity transformations. Ramesh et al.[2] investigated stagnation-point flow of Maxwell fluid towards a permeable surface in the presence of nanoparticles. Other than that, Ibrahim et al.[3] studied the nonlinear radiative heat transfer in magnetohydrodynamic (MHD) stagnation-point flow of nanofluid passed through a stretching sheet with convective boundary condition. This study was extended by many authors such as Nandy and Pop[4], Abbas et al.[5], Kumara et al.[6], Alizadeh et al.[7] and Khan et al.[8] in the effort to explore various aspects of heat transfer surrounding a stagnation point.

In the recent past, the importance of the Soret effect has attracted the attention of several researchers in many physical processes and its effect on the double diffusive convection in

---

[a] Corresponding author: fanazk1991@yahoo.com.my

[b] khairy@unimap.edu.my

porous medium. Numerical studies of magnetohydrodynamics free convection flow of an incompressible and electrically conduction fluid over a stretching surface in the presence of Soret and Dufour effects with thermophresis have been investigated by Aurangzaib[9]. The numerical results obtained show that the increase in Soret number, increases the skin friction coefficient and Nusselt number, while the Sherwood number decreases. Pal et al.[10] investigated Soret effect on convective heat and mass transfer of nanofluids over a vertical non-linear stretching/shrinking sheet in the presence of thermal radiation. They found that the skin friction coefficient and Nusselt number for shrinking sheet decreased as the Soret number increased, whereas the reverse effect are found for stretching case.

The applications of the fluid exhibiting boundary slip found in technologies such polishing of artificial heart valve and internal cavities. Bhattacharyya et al.[11] considered the MHD boundary layer slip flow and heat transfer over a flat plate. Bhattacharyya et al.[12] also studied the slip effects on boundary layer stagnation-point flow and heat transfer towards a shrinking sheet. Hady et al.[13] studied the slip effect on unsteady MHD stagnation point flow of a nanofluid over stretching sheet in a porous medium with thermal radiation.

Motivated by the aforementioned works, this paper study the behaviour of the heat and mass transfer in MHD stagnation-point flow over a permeable stretching/shrinking sheet in the presence of radiation effect, Soret effect and slip parameter. The governing partial differential equations are converted into ordinary differential equations using similarity transformation, before being solved numerically using the bvp4c function in Matlab software and shooting method in Maple software. Effects of slip parameter and Soret number are explored and discussed in detail.

2. MATHEMATICAL FORMULATION

Let us consider a magnetohydrodynamic stagnation-flow due to a stretching/shrinking sheet with internal heat generation/absorption effect, radiation effect, Soret effect and slip effect. The x-axis is taken along the direction of the continuous stretching/shrinking sheet and the y-axis is measured normal to the stretching/shrinking sheet. It is assumed that the surface is permeable and the mass flux velocity v_w with $v_w < 0$ for suction and $v_w > 0$ for injection. It is also assumed that the velocity of the stretching/shrinking velocity $u_w(x) = ax$, stagnation point flow $u_e(x) = bx$ where a and b are constants. The constant temperature at the surface $T_w(x)$ and the constant concentration at the surface $C_w(x)$ are also assumed. Under these assumptions and boundary layer approximations, the governing equations can be written as:

$$\frac{\partial u}{\partial x} + \frac{\partial v}{\partial y} = 0 \tag{1}$$

$$u\frac{\partial u}{\partial x} + v\frac{\partial u}{\partial y} = u_e \frac{du_e}{dx} + v\frac{\partial^2 u}{\partial y^2} - \frac{\sigma B_0^2}{\rho}\left(u - u_e(x)\right) \tag{2}$$

$$u\frac{\partial T}{\partial x} + v\frac{\partial T}{\partial y} = \alpha \frac{\partial^2 T}{\partial y^2} - \frac{1}{\rho C_p}\frac{\partial q_r}{\partial y} + \frac{Q_0}{\rho C_p}\left(T - T_\infty\right) \tag{3}$$

$$u\frac{\partial C}{\partial x} + v\frac{\partial C}{\partial y} = D_B \frac{\partial^2 C}{\partial y^2} + D\frac{\partial^2 T}{\partial y^2} - k_0\left(C - C_\infty\right) \tag{4}$$

where u and v are the velocity component along the x and y axes, u_e is the dimensionless velocity, T is the fluid temperature, C is the fluid concentration, v is the kinematic viscosity of

the fluid, D_B is the Brownian diffusion coefficient, D is the species diffusivity, C_p is the specific heat at constant pressure, σ is the electric conductivity of the fluid, B_0 is the applied uniform magnetic field normal to the surface of the surface of the sheet, q_r is the radiative heat flux, Q_0 is the volumetric rate of heat generation and absorption, and k_0 is the constant chemical reaction rate.

It is assumed that Equations. (1)-(4) are subject to the boundary conditions:

$$v = v_w, \ u = u_w + u_{slip}, \ T = T_w, \ C = C_w \ \text{at} \ y = 0$$

$$u \to u_e, \ T \to T_w, \ C \to C_w \ \text{as} \ y \to \infty \tag{5}$$

where $u_{slip} = L \dfrac{\partial u}{\partial y}$ is the slip velocity factor.

Referring to Brewster[14], by using Rosseland approximation, and following the papers by Ishak[15], Babu et al.[16] and Yasin et al.[17], the energy Eq. (3) can be written as

$$u \frac{\partial T}{\partial x} + v \frac{\partial T}{\partial y} = \alpha \left(1 + \frac{16 \sigma^* T_\infty^3}{3 k k^*} \right) \frac{\partial^2 T}{\partial y^2} + \frac{Q_0}{\rho C_p} \left(T - T_\infty \right) \tag{6}$$

where k is the thermal conductivity, σ^* is the Stefan-Boltzmann constant and k^* is the mean absorption coefficient.

The similarity solution of Eqs. (1), (2), (4) and (6) of the following form:

$$\psi = \sqrt{av} \, x f(\eta), \quad \theta(\eta) = \left(T - T_\infty \right) / \left(T_w - T_\infty \right),$$

$$\phi(\eta) = \left(C - C_\infty \right) / \left(C_w - C_\infty \right), \quad \eta = y \sqrt{av} \tag{7}$$

where $\psi(x, y)$ is the stream function, which is defined as $u = \partial \psi / \partial y$ and $v = -\partial \psi / \partial x$. Thus

$$u = ax f'(\eta), \ v = \sqrt{av} f(\eta) \tag{8}$$

where primes denote the differentiation with respect to η. Thus, the dimensionless parameter γ defined as

$$\gamma = -v_w / \sqrt{av} \tag{9}$$

where $\gamma > 0$ corresponds to suction and $\gamma < 0$ for injection.

The stretching/shrinking parameter, stagnation-point parameter and slip parameter defined as

$$\varepsilon = \frac{b}{a}, \quad r = \frac{b}{a}, \quad \delta = L \left(\sqrt{\frac{a}{v}} \right) \tag{10}$$

with $\varepsilon > 0$ for stretching and $\varepsilon < 0$ for shrinking.

By substituting (7) into Eqs. (2), (6) and (4), the following ordinary differential equations are obtained as follows

$$f''' + ff'' - f'^2 - M(f' - r) + r^2 = 0 \tag{11}$$

$$\frac{1}{\text{Pr}}\left(1 + \frac{4}{3}R\right)\theta'' + f\theta' + Q\theta = 0 \tag{12}$$

$$\phi'' + Sc\, f\phi' - Sc\, K\, \phi + ScSr\, \theta'' = 0 \tag{13}$$

subject to the boundary conditions

$$f(0) = \gamma, f'(0) = \varepsilon + \delta f''(0), \ \theta(0) = 1, \ \phi(0) = 1$$

$$f'(\eta) \to r, \ \theta(\eta) \to 0, \ \phi(0) \to 0 \text{ as } \eta \to \infty \tag{14}$$

The dimensionless constants Pr, Sc, M, R, Q, K and Sr denote the Prandtl number, the Schmidt number, the magnetic parameter, the radiation parameter, the heat source $(Q > 0)$ or sink $(Q < 0)$, the chemical rate parameter and the Soret number, which are defined as

$$\text{Pr} = \frac{\nu}{a}, \ \ Sc = \frac{\nu}{D_B}, \ \ M = \frac{\sigma B_0^2}{a\rho}, \ \ R = \frac{4\sigma^* T_\infty^3}{kk^*},$$

$$Q = \frac{Q_0}{a\rho C_p}, \ \ K = \frac{k_0}{a}, \ \ Sr = \frac{D(T_w - T_\infty)}{D_B(C_w - C_\infty)} \tag{15}$$

The parameters of engineering interest in heat and mass transfer are the skin friction coefficient C_f, the local Nusselt number Nu_x and the local Sherwood number Sh_x, which are defined as

$$C_f = \frac{\tau_w}{\rho u_w^2(x)}, \ \ Nu_x = \frac{xq_w}{k(T_w - T_\infty)}, \ \ Sh_x = \frac{xq_m}{D_B(C_w - C_\infty)} \tag{16}$$

where τ_w, q_w and q_m are the skin friction or shear stress, heat flux and mass flux from the sheet which are defined as

$$\tau_w = \mu\left(\frac{\partial u}{\partial y}\right)_{y=0}, \ \ q_w = -\left(\frac{\partial T}{\partial y}\right)_{y=0} + (q_r)_{y=0}, \ \ q_m = -D_B\left(\frac{\partial C}{\partial y}\right)_{y=0} \tag{17}$$

where μ is the dynamic viscosity of the fluid. By using (7), (16) and (17), we obtain

$$\text{Re}_x^{1/2} C_f = f''(0), \ \ \text{Re}_x^{1/2} Nu_x = -\left(1 + \frac{4}{3}R\right)\theta'(0), \ \ \text{Re}_x^{1/2} Sh_x = -\phi'(0) \tag{18}$$

where $\text{Re}_x = u_w(x)x/\nu$ is the local Reynolds number.

3. RESULTS AND DISCUSSION

The ordinary differential Eq. (11)-(13), subject to the boundary conditions Eq. (14) were solved numerically using a shooting method and bvp4c function. The numerical results are shown in terms of skin friction coefficient, $\mathrm{Re}_x^{1/2} C_f$, the local Nusselt number, $\mathrm{Re}_x^{-1/2} Nu_x$, the local Sherwood number, $\mathrm{Re}_x^{-1/2} Sh_x$, velocity profile $f'(\eta)$, temperature profile $\theta(\eta)$ and concentration profile $\phi(\eta)$ for different values of *Sr* and δ.

Table 1 shows the values of the local Nusselt number for different values of Prandtl number, which is compared with findings from Yasin et al.[17] and Zaimi et al.[18]. The numerical results for the skin friction coefficient, $\mathrm{Re}_x^{1/2} C_f$ are also compared with those reported by Babu et al.[16], Yasin et al.[17] and Bhattacharyya[19], as presented in Table 2. The comparisons shown in both Tables 1 and 2 are found to be in a good agreement, and thus we are confident that the present numerical method is accurate.

Figure 1 illustrated the variation of the Sherwood number $\mathrm{Re}_x^{-1/2} Sh_x$ (rate of mass transfer) with ε for different values of *Sr*. From Figure 1, it is seen that enhancing the Soret parameter tends to decrease the local Sherwood number. This behaviour is due to the fact that Soret effect produces a mass flux from lower to higher species concentration driven by the temperature gradient.

Figure 2-4 show the variation of skin friction coefficient, the local Nusselt number and local Sherwood number respectively for different values of slip parameter, δ. From Figures 2-4, it is noted that as the δ increases, the skin friction coefficient decreases and increase both the local Nusselt number and local Sherwood number. As shown in Figure 2, with the increase in slip, more fluid get permits to slip pass the plate and as a result, the flow accelerates near the plate and away from the plate, this effect diminishes whereas shear stress decreases with increasing values of slip parameter. Increases in the values of the slip parameter leads to increase in local Nusselt number as plotted in Figure 3. This is because the slip velocity mechanism will decrease the friction near the surface and thus temperature at the surface decreases, thereby increasing the heat transfer at the sheet.

From Figure 1-4, the presence of dual solution were found for certain range of shrinking case $(\varepsilon < 0)$ and the unique solution exist for the stretching case $(\varepsilon > 0)$. There is no solution when $\varepsilon < \varepsilon_c$ where ε_c is the critical value. Based on numerical computations, these critical values of ε_c are -1.12113, -1.46959 and -1.83561 for δ =0.5, 1.0 and 1.5, respectively. The velocity, temperature and concentration profiles shown in Figure 5-8 satisfy the far field boundary conditions (14) asymptotically, which support the validity of the numerical results obtained and the existence of the dual solutions.

Table 1 The values of the $\mathrm{Re}_x^{-1/2} Nu_x$ for different values of *Pr* when $Sc = M = R = Q = R = K = \lambda = 0$ and $\varepsilon = 1$

Pr	0.72	1	2	3	4	5
Zaimi et al.[18]	0.463145	0.581977		1.165246		
Yasin et al.[17]	0.463100	0.582000		1.165200		1.568100
Present results	0.463145	0.581977	0.911358	1.165246	1.379393	1.568054

Table 2 The values of the $\mathrm{Re}_x^{1/2} C_f$ for different values of γ when $Sc = R = Q = r = K = \delta = Sr = 0$, $\mathrm{Pr} = 1$, $M = 2$, and $\varepsilon = -1$.

| γ	Bhattacharyya[19]	Babu et al.[16]	Yasin et al.[17]	Present results
1			1.6180	1.618037
2	2.414300	2.41448	2.4142	2.414214
3	3.302750	3.30281	3.3028	3.302776
4	4.236099	4.23607	4.2361	4.236068
5				5.192582
6				6.162278
7				7.140055
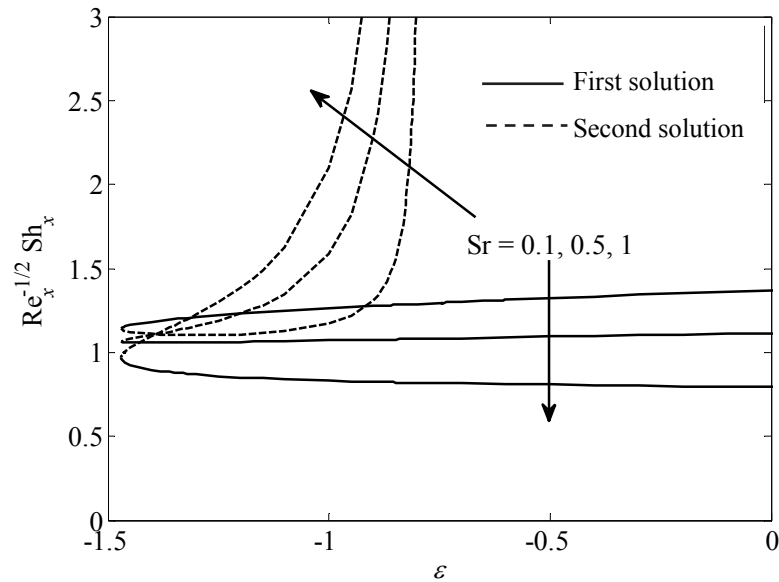
Figure 1. Variation of the Sherwood number $\mathrm{Re}_x^{-1/2}\,\mathrm{Sh}_x$ with ε for different values of Sr when $\mathrm{Pr}=1$, $Sc=1$, $M=0.2$, $R=0.1$, $Q=0.1$, $k=0.5$, $\gamma=1$, $\delta=1$ and $r=0.2$.
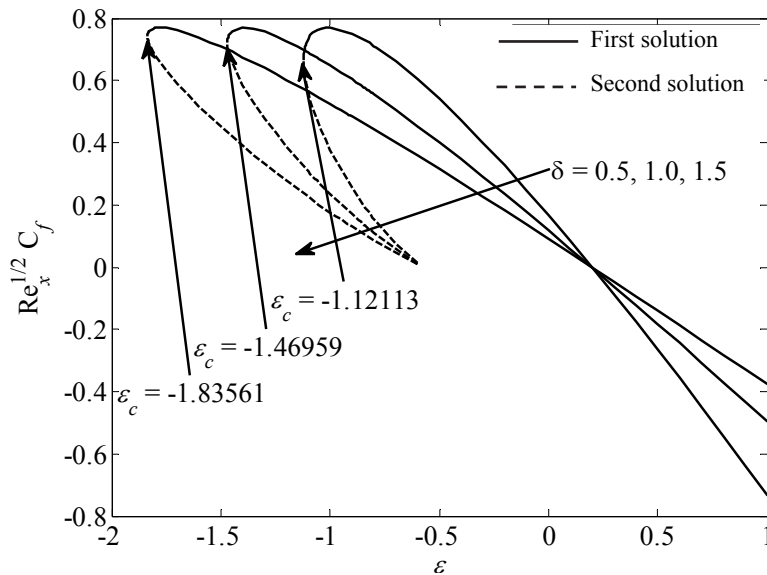
**Figure 2.** Variation of the skin friction coefficient $\mathrm{Re}_x^{1/2}\,C_f$ with ε for different values of δ when $\mathrm{Pr}=1$, $Sc=1$, $M=0.2$, $R=0.1$, $Q=0.1$, $k=0.5$, $\gamma=1$, $Sr=0.5$ and $r=0.2$.
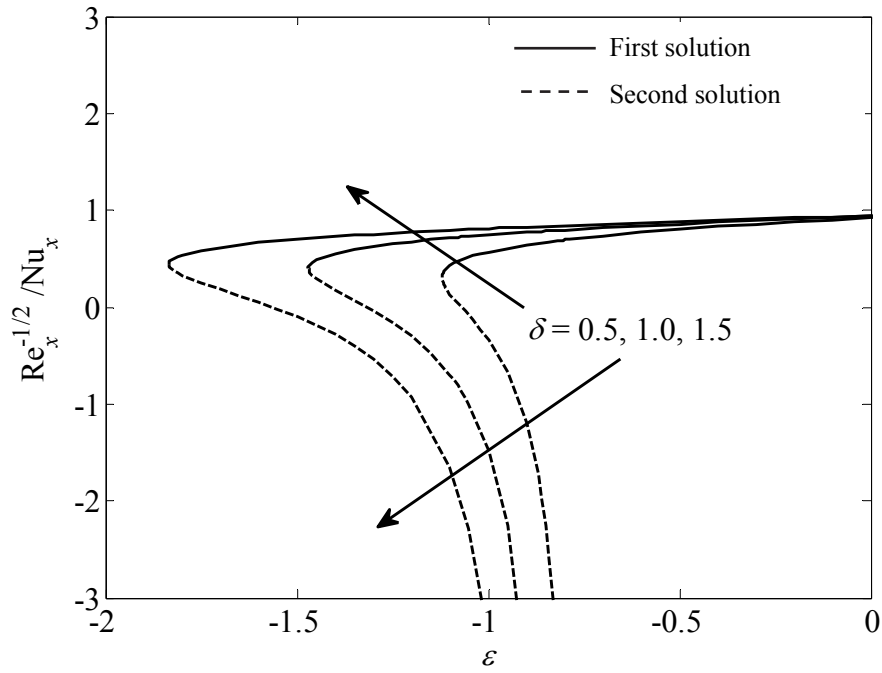
Figure 3. Variation of the local Nusselt number $\mathrm{Re}_x^{-1/2} Nu_x$ with ε for different values of δ when $\mathrm{Pr} = 1$, $Sc = 1$, $M = 0.2$, $R = 0.1$, $Q = 0.1$, $k = 0.5$, $\gamma = 1$, $Sr = 0.5$ and $r = 0.2$.
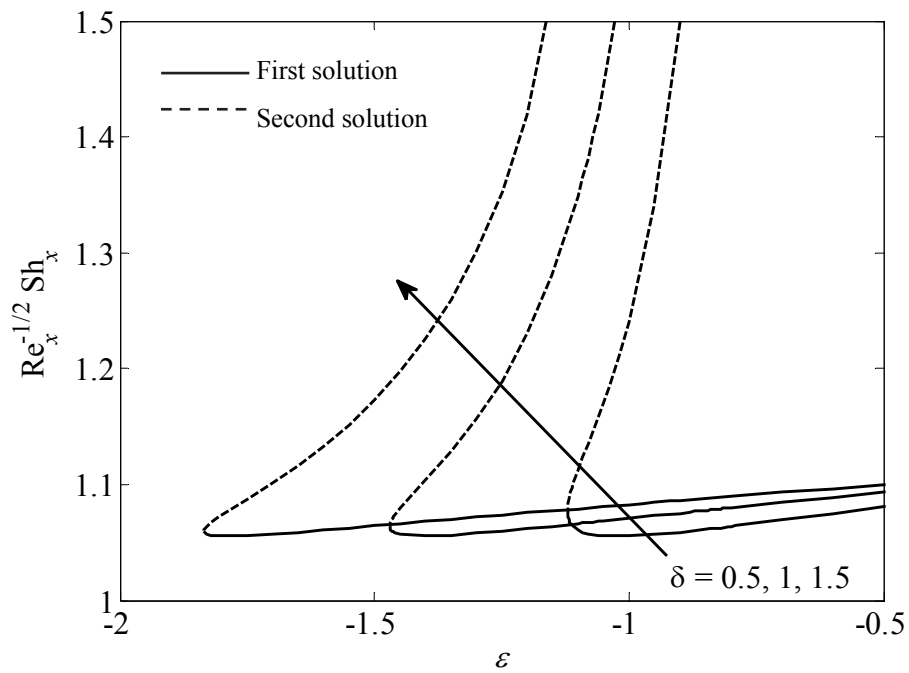
Figure 4. Variation of the Sherwood number $\mathrm{Re}_x^{-1/2} \mathrm{Sh}_x$ with ε for different values of δ when $\mathrm{Pr} = 1$, $Sc = 1$, $M = 0.2$, $R = 0.1$, $Q = 0.1$, $k = 0.5$, $\gamma = 1$, $Sr = 0.5$ and $r = 0.2$.
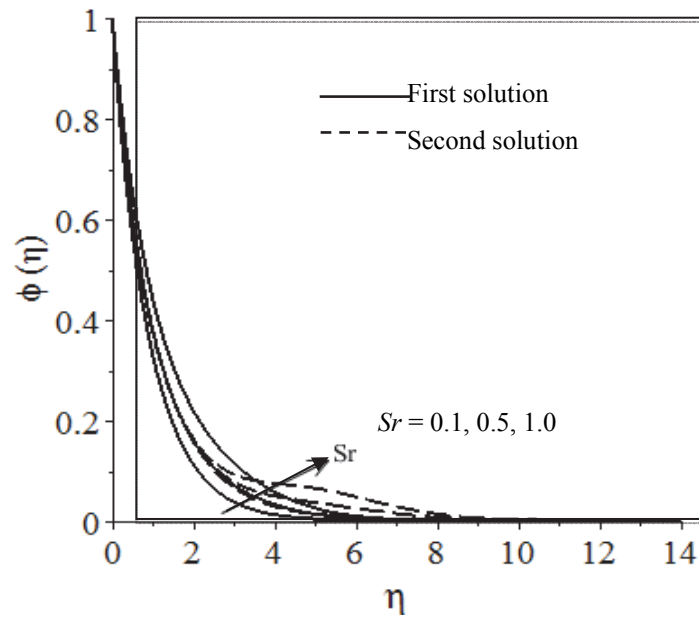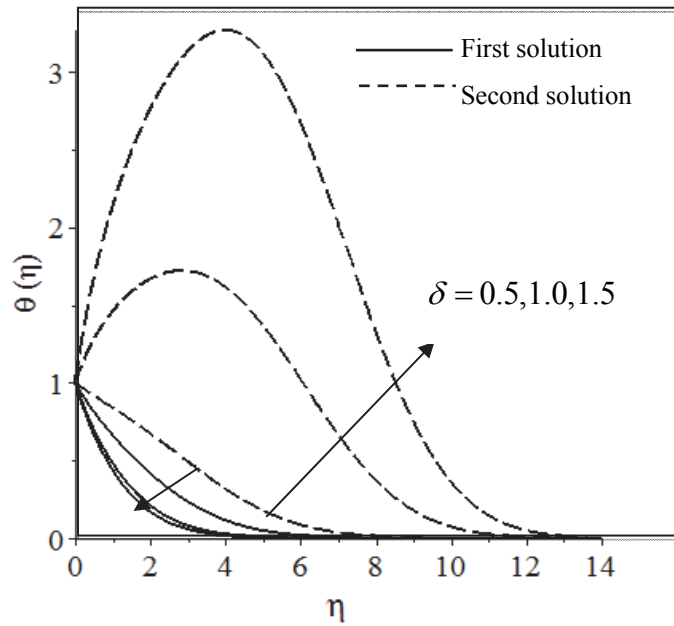
Figure 5. The concentration profiles $\phi(\eta)$ for different values of Sr when $Pr = 1$, $Sc = 1$, $M = 0.2$, $R = 0.1$, $Q = 0.1$, $k = 0.5$, $\gamma = 1$, $\delta = 1$, $r = 0.2$ and. $\varepsilon = -1.1$ (shrinking case).
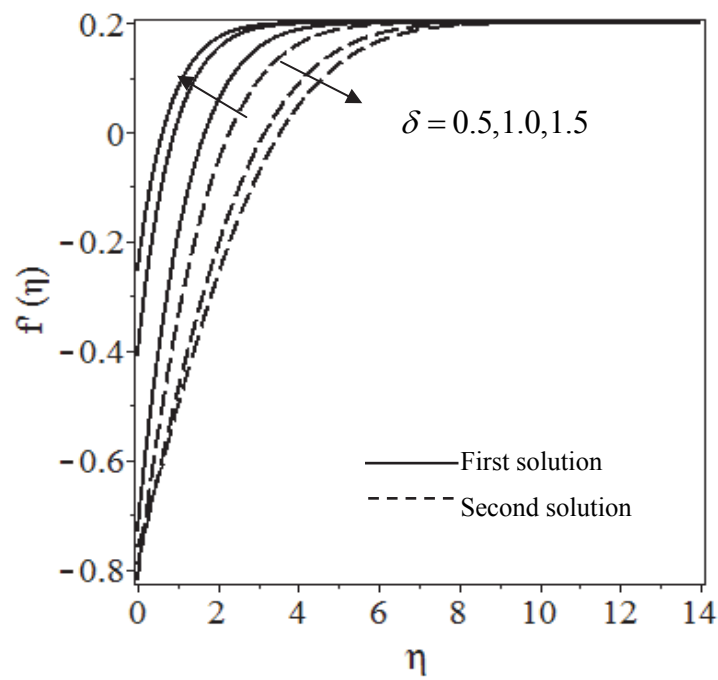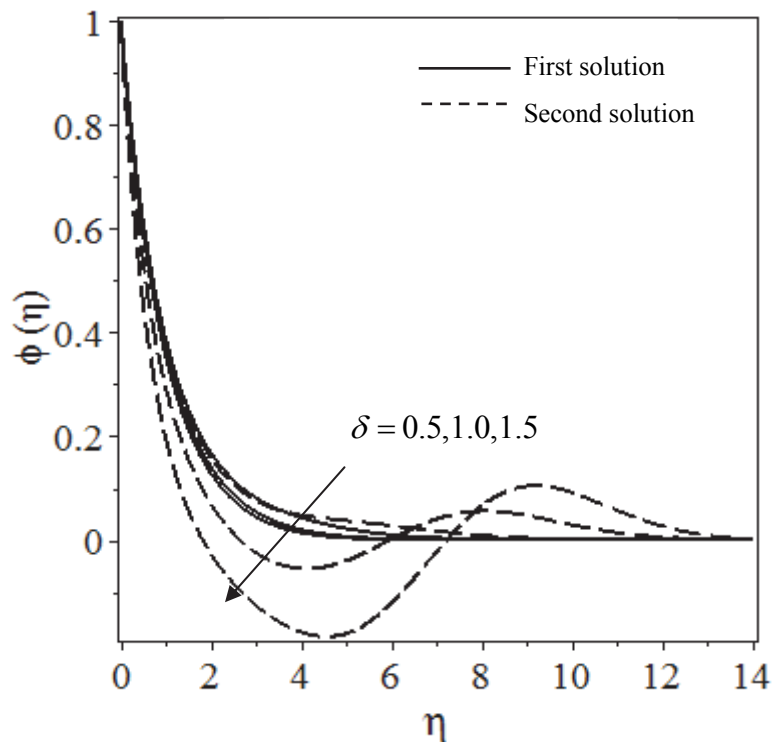

Figure 6. The velocity profiles $f'(\eta)$ for different values of δ when $Pr = 1$, $Sc = 1$, $M = 0.2$, $R = 0.1$, $Q = 0.1$, $k = 0.5$, $\gamma = 1$, $\delta = 1$, $r = 0.2$ and $\varepsilon = -1.1$ (shrinking case).

Figure 7. The temperature profiles $\theta(\eta)$ for different values of δ when $\mathrm{Pr}=1$, $Sc=1$, $M=0.2$, $R=0.1$, $Q=0.1$, $k=0.5$, $\gamma=1$, $\delta=1$, $r=0.2$ and $\varepsilon=-1.1$ (shrinking case).

Figure 8. The concentration profiles $\phi(\eta)$ for different values of δ when $\mathrm{Pr}=1$, $Sc=1$, $M=0.2$, $R=0.1$, $Q=0.1$, $k=0.5$, $\gamma=1$, $\delta=1$, $r=0.2$ and $\varepsilon=-1.1$ (shrinking case).

4. CONCLUSION

This paper presents a numerical solution of steady two-dimensional magnetohydrodynamic (MHD) stagnation-point flow over a permeable stretching/shrinking sheet with radiation effect, Soret effect and slip parameter. Dual solutions were found to exist for the certain range of shrinking case and the unique solution exist for the stretching case. From this paper, it was observed that as the Soret effect increases, the local Sherwood number decreases. When the slip parameter increased, the skin friction coefficient decreased and the local Nusselt number and local Sherwood number increased.

REFERENCES

1. K. Hiemenz, Dingler Polytech. J. **326**, 321 (1911).
2. G.K. Ramesh, B.J. Gireesha, T. Hayat, and A. Alsaedi, Alexandria Eng. J. **55**, 857 (2016).
3. W. Ibrahim, B. Shankar, and M.M. Nandeppanavar, Int. J. Heat Mass Transf. **56**, 1 (2013).
4. S.K. Nandy and I. Pop, Int. Commun. Heat Mass Transf. **53**, 50 (2014).
5. Z. Abbas, M. Sheikh, and I. Pop, J. Taiwan Inst. Chem. Eng. **55**, 69 (2015).
6. B.C.P. Kumara, G.K. Ramesh, A.J. Chamkha, and B.J. Gireesha, Int. J. Ind. Math. **7**, 77 (2015).
7. R. Alizadeh, A.B. Rahimi, and M. Najafi, Alexandria Eng. J. **55**, 37 (2016).
8. W.A. Khan, O.D. Makinde, and Z.H. Khan, Int. J. Heat Mass Transf. **96**, 525 (2016).
9. A.R.M.K. Aurangzaib, N.F. Mohammad, and S. Shafie, World Appl. Sci. J. **21**, 766 (2013).
10. D. Pal, G. Mandal, and K. Vajravalu, Appl. Math. Comput. **287**–**288**, 184 (2016).
11. K. Bhattacharyya, S. Mukhopadhyay, and G.C. Layek, Chinese Phys. Lett. **28**, 15 (2011).
12. K. Bhattacharyya, S. Mukhopadhyay, and G.C. Layek, Int. J. Heat Mass Transf. **54**, 308 (2011).
13. F.M. Hady, M.R. Eid, and M.A. Ahmed., J. Pure Appl. Math. Adv. Appl. **12**, 181 (2014).
14. M.Q. Brewster, *Thermal Radiative Transfer and Properties* (John Wiley & Sons., New York, 1992).
15. A. Ishak, Meccanica **45**, 367 (2010).
16. P.R. Babu, J.A. Rao, and S. Sheri, J. Appl. Fluid Mech. **7**, 641 (2014).
17. M.H.M. Yasin, A. Ishak, and I. Pop, J. Magn. Magn. Mater. **407**, 235 (2016).
18. K. Zaimi, A. Ishak, and I. Pop, PLoS One **9**, e111743 (2014).
19. K. Bhattacharyya, Chem. Eng. Res. Bull. **15**, 12 (2011).

APPENDIX
If any, the appendix should appear directly after the references without numbering, and on a new page.